MNRAS **000**, 1–11 (2022) Preprint 8 November 2022 Compiled using MNRAS LATEX style file v3.0

HD 42477: coupled r modes, g modes and a p mode in an A0Vnne star

D. W. Kurtz[1,2⋆], R. Jayaraman[3], P. Sowicka[4], G. Handler[4], H. Saio[5], J. Labadie-Bartz[6,7,8], U. Lee[5]

[1]*Department of Physics, North-West University, Dr Albert Luthuli Drive, Mahikeng 2735, South Africa*
[2]*Jeremiah Horrocks Institute, University of Central Lancashire, Preston PR1 2HE, UK*
[3]*Department of Physics, and Kavli Institute for Astrophysics and Space Research, M.I.T., Cambridge, MA 02139, USA*
[4]*Nicolaus Copernicus Astronomical Center, Polish Academy of Sciences, ul. Bartycka 18, 00-716, Warszawa, Poland*
[5]*Astronomical Institute, Graduate School of Science, Tohoku University, Sendai 980-8578, Japan*
[6]*LESIA, Paris Observatory, PSL University, CNRS, Sorbonne University, Université Paris Cité, 5 place Jules Janssen, 92195 Meudon, France*
[7]*Homer L. Dodge Department of Physics and Astronomy, University of Oklahoma, 440 W. Brooks Street, Norman, OK 73019, USA*
[8]*Instituto de Astronomia, Geofísica e Ciências Atmosféricas, Universidade de São Paulo, Rua do Matão 1226, Cidade Universitária, 05508-900 São Paulo, SP, Brazil*

Accepted XXX. Received YYY; in original form ZZZ

ABSTRACT

Several studies have shown that a number of stars pulsating in p modes lie between the β Cep and δ Sct instability strips in the HR Diagram. At present, there is no certain understanding of how p modes can be excited in this $T_{\rm eff}$ range. We attempt to disprove the conjecture that all such stars lying in this $T_{\rm eff}$ range are the result of incorrect measurements of $T_{\rm eff}$, or possess unseen cooler companions lying in the δ Sct instability strip – given the high binary fraction of stars in this region of the HR Diagram. Using TESS data, we show that the A0Vnne star HD 42477 has a single p mode coupled to several r modes and/or g modes. We rule out a contaminating background star with a pixel-by-pixel examination, and we essentially rule out the possibility of a binary companion δ Sct star. We model the pulsations in HD 42477, and suggest that the g modes are excited by overstable convective core modes. We conjecture that the single p mode is driven by coupling with the g modes, or that the oblateness of this rapidly rotating star permits driving by He II ionization in the equatorial region.

Key words: stars: emission-line, Be; stars: oscillations; asteroseismology; stars: individual: (TIC 294125876; HD 42477)

1 INTRODUCTION

In asteroseismology, pulsating stars are grouped into classes based on a combination of their positions in the HR Diagram and their pulsation characteristics (e.g., Kurtz 2022; Aerts 2021; Aerts et al. 2010, chapter 2). The main groups along the upper main-sequence, for pulsating stars of A–F spectral type, are the g mode pulsators, the γ Dor stars, and the p-mode and mixed p- and g-mode pulsators, the δ Sct stars. The observed and theoretical instability strips for these two groups overlap. Among B stars the main groups are the hotter p-mode and mixed p- and g-mode pulsators, the β Cep stars, and the cooler g mode pulsators, the Slowly Pulsating B (SPB) stars. The observed and theoretical instability strips for these two groups also have a small overlap.

Mixed in with β Cep and SPB stars are the classical Be stars, ranging in spectral type from late-O to early-A stars. The Be stars are the most rapid rotators found among main-sequence stars, with equatorial rotation velocities nearing breakup velocity. They have irregularly timed mass ejection episodes – or outbursts – that form circumstellar disks, which are evidenced by emission lines in their spectra. They are also generally nonradial g mode pulsators, and this pulsation behaviour is somehow related to the outbursts (e.g., Kurtz et al. 2015), although this is not yet fully understood.

For some time, observations have shown that there are stars in all the OBAF pulsation classes – γ Dor, δ Sct, SPB, and β Cep – that appear to lie outside of their respective theoretical instability strips. Degroote et al. (2009), in a study of B stars observed by the *CoRoT* mission, suggested a new class of pulsating variables in the spectral type range between the SPB and δ Sct instability strips, i.e., late-B to early-A spectral types. They also noted that the highest amplitude SPB stars show both nonlinearities, in the form of combination frequencies, and low frequencies that show excess amplitude after the principal pulsation frequencies have been pre-whitened. Such behaviour indicates amplitude and/or frequency

⋆ E-mail: kurtzdw@gmail.com

modulation as a consequence of limited lifetimes for these modes. They suggested that this is caused by nonlinear resonant mode locking. Other possibilities are that the low frequencies in these stars, in addition to g modes, are also the result of closely spaced, unresolved, or only partially resolved r mode frequencies (see Saio et al. 2018), and stochastically driven modes (Bowman et al. 2019, 2020).

Bowman & Kurtz (2018) extracted 983 δ Sct stars with 4 yr of data from the 200 000 stars observed by *Kepler*. They found a significant number of δ Sct stars pulsating in p modes whose temperatures are higher than the theoretical blue edge of the δ Sct instability strip, as calculated by Dupret et al. (2004) and Grigahcène et al. (2005). That edge is often presented as the theoretical hot boundary for these stars, but this depends on the value of the mixing-length chosen for the models (Houdek & Dupret 2015, Bowman & Kurtz 2018). However, no choice of mixing length produces a blue border that encompasses all of the δ Sct stars.

This was shown by Murphy et al. (2019) in a thorough discussion of pulsator fraction of δ Sct stars across the instability strip and up to $T_{\rm eff}$ = 10 000 K. In a sample of 15 000 *Kepler* A and F stars, they found δ Sct stars hotter than the blue edge and argued statistically that these cannot be accounted for by uncertainties in $T_{\rm eff}$. They did discuss the binary fraction among A stars, but did not address the question whether all the δ Sct stars hotter than the theoretical blue border may be binaries that include a cooler δ Sct star. Moe & Di Stefano (2017, figure 38) show that for stars of $\sim 2-3\,{\rm M}_\odot$ most have companions with orbital periods greater than 2 d, and with mass ratios $q > 0.1$, with more than 40 per cent of those having mass ratios $q > 0.3$. Both of these numbers increase with higher main-sequence masses and hotter main-sequence $T_{\rm eff}$.

Using the phase modulation technique (PM), Murphy et al. (2018) found 341 non-eclipsing binaries with $P_{\rm orb} > 20$ d in a sample of 2224 A and F stars in the *Kepler* data. About 7 per cent of those stars were "PB2", meaning pulsating binary stars for which both stars pulsate and the pulsation frequencies are stable frequency references for the PM method. Thus there is a significant fraction of δ Sct stars to be found in binary systems where both stars are δ Sct. By inference there are also primary stars hotter than the blue border with somewhat cooler δ Sct secondaries. It is therefore important to examine whether all of the δ Sct stars hotter than the theoretical blue border may be binaries with a cooler δ Sct secondary.

Bowman & Kurtz (2018) also found that g mode pulsations exist in δ Sct stars at temperatures higher than the theoretical γ Dor g-mode instability strip, confirming the discovery made by Grigahcène et al. (2010) from the initial quarters 0 and 1, comprising a 44.5-d time span, of the *Kepler* mission. But this, too, must be examined cautiously. Their study and almost all others did not consider r modes, and most studies have not carefully distinguished combination frequencies due to mode coupling from g mode frequencies, although this problem is widely recognised and discussed.

These observations of the B and A stars with *CoRoT* and *Kepler* give rise to important questions. The primary driving mechanisms across the upper main-sequence stars are the κ-mechanism, operating in the He II ionization zone for the δ Sct stars, and in the ionization zone of the Fe-peak elements for the B stars. In addition, convective blocking is thought to be the dominant driving mechanism in γ Dor stars (Dupret et al. 2005). However, if both p modes and g modes are found in stars outside of the theoretically understood instability strips, then further developments in our understanding of driving and damping in main-sequence B, A and F stars is needed.

Prior to searching for modifications to pulsation models, we need to be sure that the observations demand that. How secure are the temperatures that show p-mode pulsators to lie between the SPB and δ Sct instability strips? How confident can we be in determining which star represents the true origin of the observed pulsations, given the high incidence of binarity on the upper main-sequence? Given the exquisite precision of *Kepler* and TESS data, which have noise levels in amplitude typically around 1 μmag and 10 μmag, respectively, how likely is it that some frequencies for a given star originate in contaminators?

The *Kepler* mission field-of-view was intentionally chosen to be out of the crowded Milky Way plane for the primary goal of exoplanet detection. A consequence was that few B stars were observed, although over 1000 δ Sct and γ Dor stars were observed for the full 4-yr time span of the main mission. Now, the successor to the *Kepler* mission, the Transiting Exoplanet Survey Satellite, TESS, has been surveying almost the entire sky with "Sectors" of length 27 d. Near the poles of the TESS orbit, some stars have been observed for up to 1 yr. Given that TESS has now tiled the sky twice, there exist over two full years of data for some stars near the celestial poles. Most importantly, TESS is observing bright, nearby stars for which determination of fundamental parameters, e.g., $T_{\rm eff}$, $\log g$, distance, luminosity and metallicity, can be done to high accuracy.

Balona & Ozuyar (2020) carried out a large-scale survey of about 50 000 stars observed by TESS. They found a large number of p mode pulsators in the temperature range between the β Cep and δ Sct instability strip and referred to them as "Maia" variables for historical reasons. However, it is now known from *Kepler* observations that the star Maia itself does not pulsate (White et al. 2017).[1] In their work, Balona & Ozuyar recognised two problems with making conclusions from the apparent positions in the HR Diagram of this suggested new class of pulsating variable stars. There could be errors in the positions caused by uncertainties in $T_{\rm eff}$, and the stars may be binary. Balona & Ozuyar state: "They could possibly be composite objects consisting of a non-pulsating B star and a δ Sct star", but they do not follow up on this possibility and test individual stars in their sample. A third problem they do not mention, but that is important, is that of background contaminating stars.

Both Balona & Ozuyar (2020) and Bowman & Kurtz (2018) used spectroscopic temperatures in their arguments that there are p mode pulsators in the range between the β Cep and δ Sct stars. They gave good arguments that the uncertainties in $T_{\rm eff}$ are sufficiently low that the stars are neither β Cep nor δ Sct stars that are incorrectly plotted in the HR Diagram due to a poorly estimated value of $T_{\rm eff}$. As mentioned above, Murphy et al. (2019) made statistical arguments that errors in $T_{\rm eff}$ cannot explain the δ Sct stars hotter than the theoretical blue border. Thus, incorrect $T_{\rm eff}$ is not the source of the p mode pulsators found to lie in the region between the β Cep and δ Sct stars.

The problem of binarity as an explanation for p mode pulsators between the δ Sct and β Cep instability strips is not well-examined. The binary fraction for B stars is high – essentially 100 per cent (Moe & Di Stefano 2017) – and many B star companions could be A stars in the δ Sct instability strip. A conjecture for the p mode pulsators found between the β Cep and δ Sct instability strips could be that these stars all have unrecognised δ Sct companions, whether in short period binaries or wide ones. Neither TESS, nor previous observations, can resolve this. To disprove the conjecture that all of the p mode pulsators between the β Cep and δ Sct theoretical

[1] A prototype that is not a member of its class calls for a different name for these stars.

instability strips are stars with fainter δ Sct companions, all that is needed is proof that one star in the correct temperature range between those two instability strips pulsates with at least one p mode.

This requires proving that the pulsations are not in a companion or background star. This is an observationally difficult, time-consuming challenge, which is why it has not yet been done. In this work, we attempted to prove that the coupled p mode and low-frequency r modes and g modes seen in the amplitude spectrum of the A0Vnne star HD 42477 all originate in that star, and cannot be in an undetected companion or contaminating star. We have strongly constrained the parameter space for a putative companion, but have not fully ruled out a possibly still-undetected cool δ Sct – γ Dor secondary, although that is highly unlikely, given the Be nature of HD 42477.

Thus, we have not succeeded in proving the suggestions of Balona & Ozuyar (2020), Murphy et al. (2019), Bowman & Kurtz (2018), Degroote et al. (2009), and others that there definitely are p mode pulsators across late-B to early-A spectral types. Balona & Ozuyar (2020) make a statistical case for the fraction of stars pulsating with p modes peaking in the β Cep and δ Sct instability strips, as determined theoretically, but that there exists a lower fraction of p mode pulsators across the intermediate temperatures along the main-sequence (see their figure 7). They did not, however, observationally rule out the possibility that all of these stars have cooler δ Sct companions.

Theoretically, Szewczuk & Daszyńska-Daszkiewicz (2017) recalculated the instability strips of upper main-sequence stars with masses from $2 - 20\,M_\odot$. They examined modes of degree $\ell \leq 4$ with the effects of rotation included, which shifts the boundary of the SPB instability strip to lower temperature. They conjectured that this, combined with surprisingly high frequencies for rapid rotators, may explain the p mode pulsators that appear to lie between the SPB and δ Sct instability strips. Salmon et al. (2014) also conjectured that gravity darkening in rapid rotators, which can make equator-on stars appear cooler, as well as higher frequencies from sectoral prograde dipole modes, can explain apparent g mode pulsators observed in the SPB – δ Sct gap in NGC 3766 (Mowlavi et al. 2013).

A similar problem is the existence of hot γ Dor stars with temperatures well above the theoretical hot border of the instability strip for those stars. Kahraman Aliçavuş et al. (2020) studied 24 hot γ Dor (or candidate) stars spectroscopically, testing whether they could be explained as binary stars with a hotter δ Sct and cooler γ Dor star, or whether they could be rapidly rotating SPB pulsators where gravity darkening makes them look cooler. They concluded that the number of hot γ Dor stars is low, but real. These stars have surface convective zones too shallow to plausibly drive pulsations by convective blocking (Guzik et al. 2000), suggesting a need for an additional driving mechanism in at least some A stars with g mode pulsations.

HD 42477 addresses another interesting question. The Be phenomenon of emission lines and outbursts in rapidly rotating B stars does not have a universally accepted explanation. To address this, Labadie-Bartz et al. (2022, 2017) have made major studies of Be stars with ground-based observations from the Kilodegree Extremely Little Telescope (KELT), and from TESS. From analyses of 432 TESS Be stars, they found that almost all Be stars show multiple peaks in amplitude spectra in the $0.5 - 4\,d^{-1}$ range, the usual range for g modes. They note that closely spaced groups of frequencies are a common feature in 85 per cent of their 432 stars. Kurtz et al. (2015) showed that these frequency groups are often a result of combination frequencies from nonlinear coupling of pulsation modes.

Van Reeth et al. (2016) found in a study of *Kepler* γ Dor stars that the pulsation modes are a combination of g modes and r modes – global Rossby waves. Saio et al. (2018) found r modes in B and A stars, including an outbursting Be star. Lee & Saio (2020) then showed how a rotating convective core can couple to g modes in the radiative envelope of a $2\,M_\odot$ model, thus providing an explanation for the commonly observed low frequencies seen in amplitude spectra of B and A stars that are close to their respective inferred rotation frequencies.

Assuming that the pulsations are in the A0Vnne star, we show in this paper a 9900 K model of HD 42477 explaining the low frequencies as g modes and r modes, and we suggest that r modes are a common feature in Be stars. We also show in HD 42477 that the low frequency r modes and g modes are nonlinearly coupled to the high frequency p mode. It is that coupling that shows the p mode is in the same star as the g modes and r modes. We suggest that this coupling of the p mode to the g modes – for which there is theoretical understanding of the excitation – may provide the boost in driving needed to understand how p modes can be excited in the temperature range between the β Cep and δ Sct theoretical instability strips. Previous calculations of the boundaries of those strips have not considered such a boost from coupled modes.

Finally, there are the questions of whether a background star or an orbital companion could be the source of both the g mode and r mode low frequencies and the high frequency p mode in HD 42477. We have examined both these questions. Because the TESS pixel size is 21 arcsec, and the masks encompass several to many pixels, the potential for contamination in the TESS data is high. This is an important consideration, given the high precision of the data, typically with amplitude uncertainties in the several μmag range for brighter stars. Some δ Sct stars are known to show g modes, r modes and p modes in the same star, hence we examine the TESS field pixel-by-pixel and demonstrate that the frequency spectrum of HD 42477 discussed in this work does not originate in a contaminating star.

We then look carefully at spectra we have obtained of HD 42477 and find no evidence of an orbital companion of the brightness of an A star with $v \sin i \leq 100\,\mathrm{km\,s^{-1}}$. We are not able, however, to rule out a more rapidly, somewhat cooler companion which would lie near the red border of the δ Sct and γ Dor instability strips.

2 HD 42477

HD 42477 (TIC 294125876, HR 2191) is classified A0Vnne (Cowley et al. 1969), meaning an A0 main-sequence star with very broad spectral lines, implying rapid rotation, and emission lines[2]. Hence, this is a Be star at the cool end of the range. Cowley et al. (1969) also note "sharp K line superimposed on hazy one", which is consistent with a Be circumstellar disk; they further note "Si:", which signifies marginal enhancement of Si. It is unlikely that this star is a marginal Ap star with weak abundance anomalies, as both magnetic (ApSi) and non-magnetic (HgMn) Ap stars rotate much more slowly than HD 42477, and generally show rotational light variations, which are not present for HD 42477.

Labadie-Bartz et al. (2017) reported KELT photometry of 610 known Be stars, of which HD 42477 was one. The KELT photometry

[2] The "n" in spectral classes is an abbreviation of "nebulous" – referring to the broadening of the spectral lines in classification spectra.

for this bright star was saturated, so they made no report on its photometric variability. We have carefully re-examined the KELT data and find that the p mode is detectable. Then, Labadie-Bartz et al. (2022) analysed TESS photometry for 432 Be stars in TESS Sectors 1 – 13. They, too, noted stars with high frequencies in the δ Sct range, but did not include HD 42477, since it was not first observed by TESS until Sector 33. Hence, this paper, which utilizes TESS data, is the first to show and discuss the photometric variability of this star.

3 FREQUENCY ANALYSIS OF HD 42477

HD 42477 was observed by TESS in Sector 33, then again in Sectors 43–45; all observations were conducted at 2-min cadence. The data are available in both SAP (simple aperture photometry) and PDCSAP (presearch-data conditioning SAP); we used the S33 PDCSAP data for modelling, and the S43–45 PDCSAP data for frequency analysis, after having converted intensity to magnitudes. The S43–45 data have a time span of 75.46 d, with a centre point in time of t_0 = BJD 24559512.40014. These data comprise 48060 data points, after clipping 28 outliers, probably caused by cosmic rays. There are ∼2-d gaps in the data at the time of perigee. The TESS orbit is a lunar-synchronous eccentric orbit, with an orbital period of half the sidereal orbital period of the moon. This keeps the satellite from being perturbed significantly at apogee, and allows for higher bandwidth data downloads at perigee. The gaps in the data thus come during the data transfers. Fig. 1 shows the light curve of the Sector 44 data, where low-frequency variability is obvious.

The S43–45 data were analysed using a fast Discrete Fourier Transform (Kurtz 1985) to produce the amplitude spectra shown in Fig. 2. Thirteen significant resolved peaks were identified and are listed in Table 1. The 3 low-frequency peaks in the $1 - 3\,\mathrm{d}^{-1}$ range do not have any harmonic relationship. There are 10 frequencies in the δ Sct pulsation range between $13 - 40\,\mathrm{d}^{-1}$. Table 1 demonstrates that there is one p mode pulsation frequency, labelled ν_4, and there exist 8 other frequencies in the p mode range that are consistent with combinations of ν_4 with the 3 resolved low-frequency peaks – ν_1, ν_2 and ν_3. One other frequency listed in the table is a harmonic of ν_4. Importantly, the presence of combination frequencies between the p mode and the low frequency peaks demonstrates that the δ Sct p mode pulsation is in the same star that produces the low frequency peaks.

4 THE LOW FREQUENCY G MODES AND R MODES

Because the low frequencies are not harmonic, we rule out both binary and spot light curves as the source of these peaks in the amplitude spectrum, as well as for the variability seen by eye in Fig. 1. In a combined analysis of all the data from Sectors 43–45, pre-whitening all the frequencies presented in Table 1 yields some residual amplitude at these frequencies, as can be seen in the bottom panel of Fig. 2. This indicates amplitude modulation of the r modes or g modes, or beating in unresolved modes on a timescale of months. This amplitude modulation is clearly visible in Fig. 3.

The single p mode pulsation peak and its exactly-calculated combinations and harmonic in the δ Sct frequency range are all removed in the prewhitening, as shown in the bottom panel of Fig. 2. The small residual peaks discernible in the p mode range after this pre-whitening are caused by the amplitude modulation of the coupled modes.

The behaviour of the low-frequency modes is unusual in this star. The upper main-sequence stars presented in Saio et al. (2018) show a dense hump of r mode peaks that are unresolved, whereas HD 42477 has only a few low frequency peaks. To examine the hypothesis that these observed low frequencies in HD 42477 are the result of both g modes and r modes, we modelled the pulsations.

Even though we have shown that all the modes arise in the same star, we must evaluate the possibility that these pulsations could arise from a background contaminator (and not the A0Vnne star HD 42477), or an orbital companion that is a cool δ Sct–γ Dor hybrid star. These important tasks have not previously been done for any p mode pulsator that lies between the β Cep and δ Sct instability strips. The following two sections address these issues.

5 PIXEL-BY-PIXEL EXAMINATION

For bright stars such as HD 42477, the optimal apertures chosen by the Science Processing Operations Center (SPOC) PDC pipeline consist of many pixels, giving a risk of contamination from other objects. We downloaded the Target Pixel File (TPF) of HD 42477 from the Barbara A. Mikulski Archive for Space Telescopes (MAST)[3] and examined it using tools from the Python package `lightkurve` (Lightkurve Collaboration et al. 2018). Fig. 4 shows the TPF plot, with nearby Gaia targets up to 8 magnitudes fainter overplotted. We can see that all objects within this field are much fainter than our target and should not be significant sources of contamination. This is also reflected in the `CROWDSAP` keyword value, which characterizes the ratio of flux from the target to the total flux in the aperture; this parameter has a value > 0.997 for all four sectors of data. Such a high value for this parameter suggests that any flux contribution from other sources is negligible.

While this was reassuring, we sought to ensure that there was no contribution from other sources in the TPF and conducted a pixel-by-pixel analysis of the TPF. First, we examined each pixel to choose a mask in order to extract a light curve of sources identified in the aperture. Additionally, we also extracted a raw light curve for HD 42477 using a much smaller aperture mask than the one used by the SPOC pipeline (31 pixels in the pipeline mask versus 11 in our chosen mask) to minimise any possible contamination. It is important to note that HD 42477, with TESS magnitude $T = 6.01$, is beyond the saturation level of TESS, which is about $T \leq 6.8$ (Sullivan et al. 2015)[4]. The CCDs in the TESS camera are able to conserve charge from even very saturated stars by spreading the excess charge across adjacent pixels in the CCD column, which we took into account when creating a new aperture mask for the target.

We identified two variable sources at positions corresponding to stars number 5 and 7 in Fig. 4. Star 5 is a $G = 10.34$ mag F2V star, with the designation HD 253085. Star number 7 is a $G = 11.90$ mag star, with designation Gaia DR3 3344372393516924160 (hereafter referred to as Gaia160). Gaia160 has an unknown spectral type; however, Bai et al. (2019) computed $T_{\rm eff} = 7700 \pm 400$ K. On the other hand, Gaia DR3 provides a $T_{\rm eff} = 9570^{+65}_{-60}$ K, with a $BP - RP$ colour of 0.58 (Gaia Collaboration et al. 2022). The colour agrees with the $T_{\rm eff}$ presented in Bai et al. (2019), suggesting a late-A or early-F star; the $T_{\rm eff}$ does not agree with this interpretation, however, suggesting a very early A star, if we assume that this is on the main sequence. Nevertheless, the key result for this star is that

[3] `http://archive.stsci.edu`

[4] The saturation level of a pixel is about 200 000 e^-.

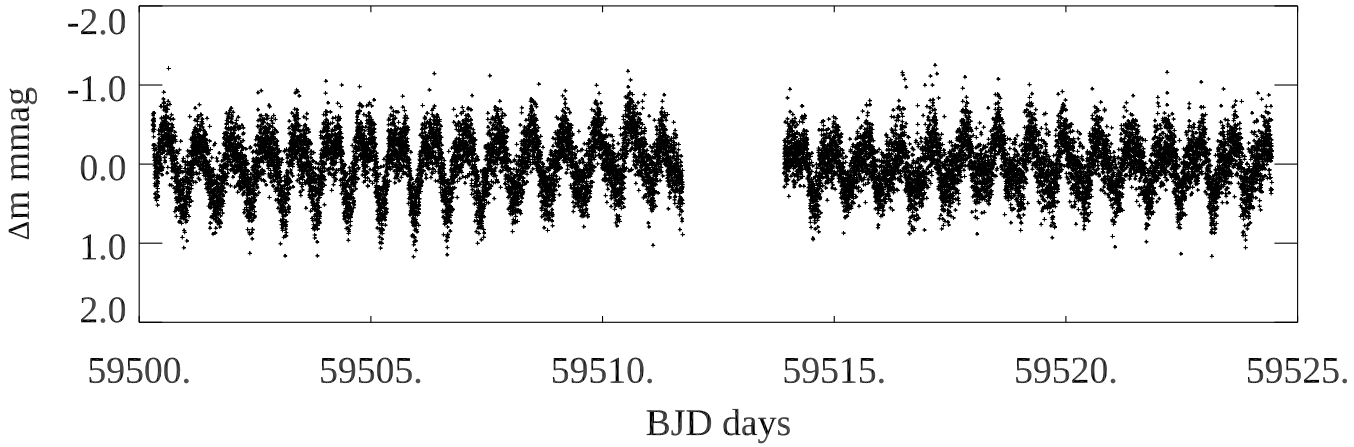

Figure 1. The light curve of HD 42477 obtained by TESS in 2-min cadence in Sector 44. The ordinate scale is Barycentric Julian Date – 240 0000.0. The low frequency variations are clear. The other Sectors look similar; only this one is shown for reasons of scale.

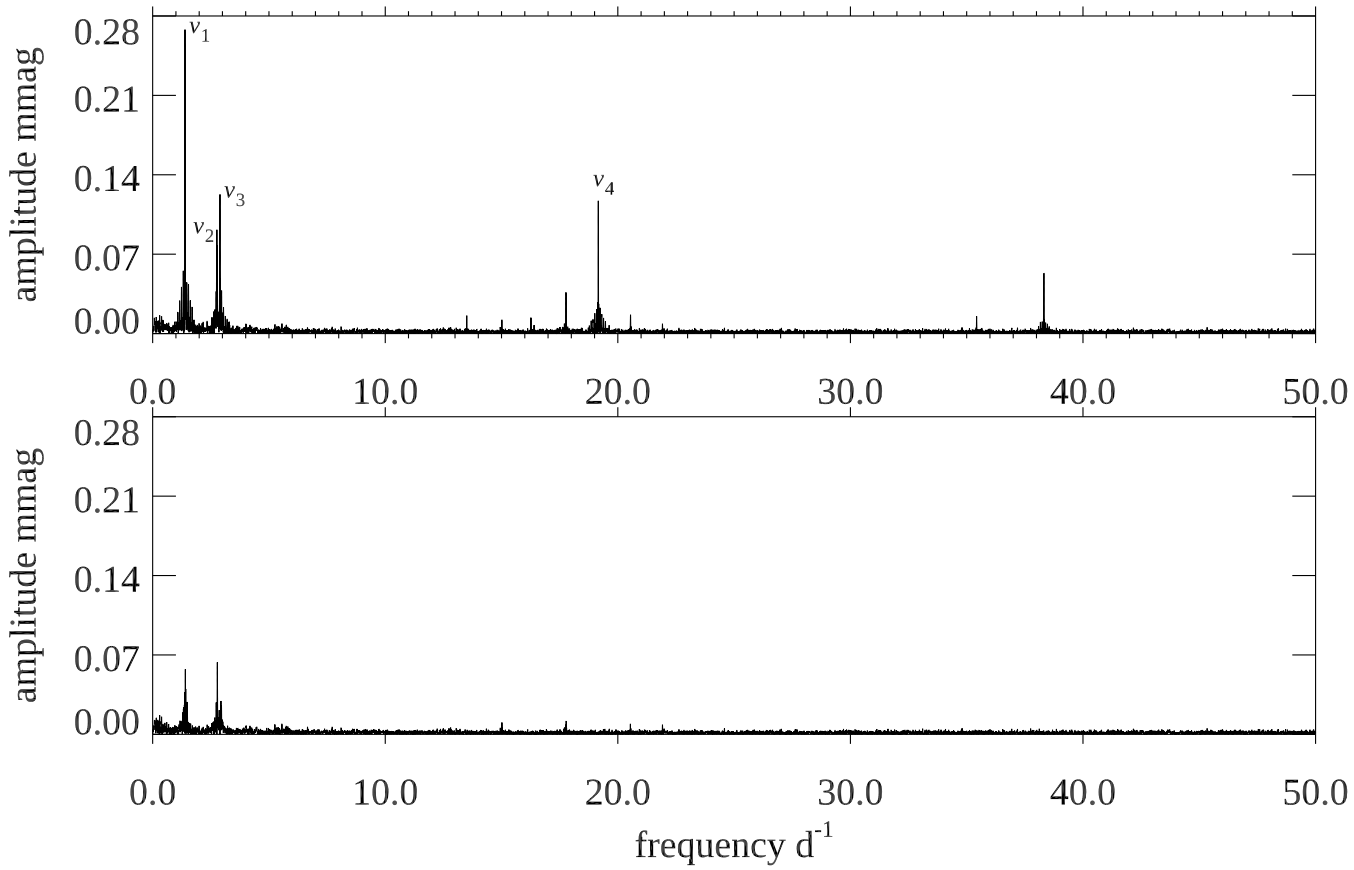

Figure 2. Top: An amplitude spectrum of the Sector 43–45 data for HD 42477, showing the four identified mode frequencies, and other combination frequencies and a harmonic in the p mode frequency range. Bottom: an amplitude spectrum of he residuals after pre-whitening the 4 mode frequencies and their exact combinations. The residual amplitude at low frequency is caused by amplitude modulation of the low frequencies, which contribute to some modulation of the combination frequencies.

Table 1. A non-linear least squares fit of the frequencies derived from S43–45 for HD 42477. The zero point for the phases is t_0 = BJD 24559512.40014. Note that there is only one independent p mode pulsation frequency at $\nu_4 = 19.16001\,\mathrm{d}^{-1}$. The last column shows the difference between the derived frequency and an exactly calculated frequency from the combination identifications in column 1, divided by the Rayleigh frequency resolution for the S43–45 data set of $0.013\,\mathrm{d}^{-1}$, thus demonstrating the frequency matches to the identifications.

	frequency d^{-1}	amplitude mmag ±0.0014	phase radians	$\Delta\nu/\sigma$
ν_1	1.39026 ± 0.00004	0.2678	−0.213 ± 0.005	
ν_2	2.76160 ± 0.00011	0.0884	−2.169 ± 0.016	
ν_3	2.89400 ± 0.00009	0.1191	−1.518 ± 0.012	
$\nu_4 - 2\nu_3 - \nu_2$	13.50479 ± 0.00068	0.0159	−1.080 ± 0.097	0.0
$\nu_4 - \nu_2 - \nu_1$	15.01599 ± 0.00081	0.0124	−2.783 ± 0.115	−0.6
$\nu_4 - \nu_3$	16.26642 ± 0.00075	0.0135	−2.644 ± 0.106	0.0
$\nu_4 - \nu_2$	16.39813 ± 0.00147	0.0069	2.906 ± 0.207	0.0
$\nu_4 - \nu_1$	17.77253 ± 0.00028	0.0361	1.063 ± 0.040	−0.2
ν_4	19.16001 ± 0.00009	0.1166	0.164 ± 0.012	
$\nu_4 + \nu_1$	20.54661 ± 0.00065	0.0156	−1.609 ± 0.091	0.3
$\nu_4 + 2\nu_1$	21.91939 ± 0.00123	0.0082	1.978 ± 0.174	1.6
$2\nu_4 - \nu_3$	35.42660 ± 0.00068	0.0147	0.082 ± 0.097	0.0
$2\nu_4$	38.32018 ± 0.00019	0.0534	2.941 ± 0.027	0.0

it is likely in the instability strip and could potentially contaminate the light curve of HD 42477 with putative high-amplitude pulsations. Finally, there is a $G = 13$ star almost exactly between Gaia160 and HD 253085 (star 9 in Fig. 4, with designation Gaia EDR3 3344373802266195200, which we abbreviate to Gaia200). This star was also investigated for any possible pulsations, but due to its comparatively faint magnitude, we focused on the other two stars for our analysis.

We extracted raw light curves using the apertures shown in Fig. 5 and corrected them using Cotrending Basis Vectors within `lightkurve`. The light curves for HD 42477, HD 253085 and Gaia160 are shown in the three middle panels of Fig. 5: HD 42477 in red (A), HD 253085 in orange (B) and Gaia160 in blue (C). The right-hand side plots show amplitude spectra of these light curves calculated from 0 to 40 d^{-1}.

The amplitude spectrum calculated using the PDCSAP light curve (pipeline aperture of 31 pixels shown in white) is shown in grey in the background of each amplitude spectrum plot. The high frequencies beyond 15 d^{-1} clearly originate in HD 42477 only, while low-frequency variability is present in all three stars. The bottom 3-panel plot of Fig. 5 shows a zoom-in into the frequency ranges of interest. In the low frequency range, it is evident that the frequencies are very close. The two highest amplitude frequencies of HD 253085 are 1.018325(93) d^{-1} and 1.180372(96) d^{-1}, and they do not overlap with any of the frequencies of HD 42477. For Gaia160 the two highest amplitude frequencies are 2.729944(21) d^{-1} and 1.365009(56) d^{-1}, which appear to be harmonically related. These two are close to ν_2 and ν_1 of HD 42477, respectively, but still are independent frequency modes, given that they are separated by more than the Rayleigh frequency resolution of the entire data set. Finally, while this is not shown in Figure 5, Gaia200 exhibits a significant peak at 4.92614(43) d^{-1}, which is not near any of the other frequencies we have investigated. This suggests it is unlikely to affect our analysis.

With this analysis, we have shown that the p mode frequency originates from within HD 42477, and that the combination terms of this frequency with the low-frequency g and r modes show that these all arise from this star. The contaminating stars are not the source of any of these frequencies, and the variability of the two nearby stars is intrinsic and not due to light spilled over from pixels saturated by HD 42477.

6 SPECTROSCOPIC SEARCH FOR A BINARY COMPANION

We tested for the presence of spectral lines of a binary companion to allow us to test whether the pulsations observed in the TESS light curve of HD 42477 originate in that star, and not in a fainter A-F star binary companion. Such a star could itself show p modes, g modes and r modes. Because Be stars are thought to have been spun up by mass transfer from a companion at an earlier stage of their evolution, we do not necessarily expect a close main-sequence companion. However, a wide main-sequence companion that would not have influenced, or been perturbed by earlier mass transfer in an inner pair, needs to be ruled out. The presence of any compact companion, such as a white dwarf, is not relevant in this context, as such a star would be too faint to contribute to the total light, and would not have the observed pulsation frequencies. We note that the Gaia DR3 RUWE (renormalised unit weight error) value for HD 42477 is 1.079, so this star is not an obvious astrometric binary.

To evaluate the presence of a companion, we examined 2 high-resolution spectra from the Be star spectra (BeSS) database[5] (Neiner et al. 2011), and we obtained 12 high-resolution (R∼53000) high signal-to-noise ratio (∼300 − 400; $t_{exp} = 1800$ s) echelle spectra with the NRES instrument attached to the 1-m telescopes at the Wise, CTIO, and McDonald observatories operated by LCOGT (Brown et al. 2013). Spectral regions including prominent absorption lines (e.g. Fe II 5169 Å, Hβ) in the NRES spectra were searched for the presence of line-profile variations by phasing the mean-subtracted residuals to ν_1, ν_2 and ν_3. However, with only relatively few observations, this test was inconclusive. The spectra were also searched for the presence of a companion by means of a comparison with synthetic spectra. The latter were computed using the `SPECTRUM` code (Gray & Corbally 1994), using $T_{\rm eff} = 10000$ K, $\log g = 3.5$ and $v \sin i = 220\,\mathrm{km\,s^{-1}}$. The effective temperature was

[5] http://basebe.obspm.fr/basebe/

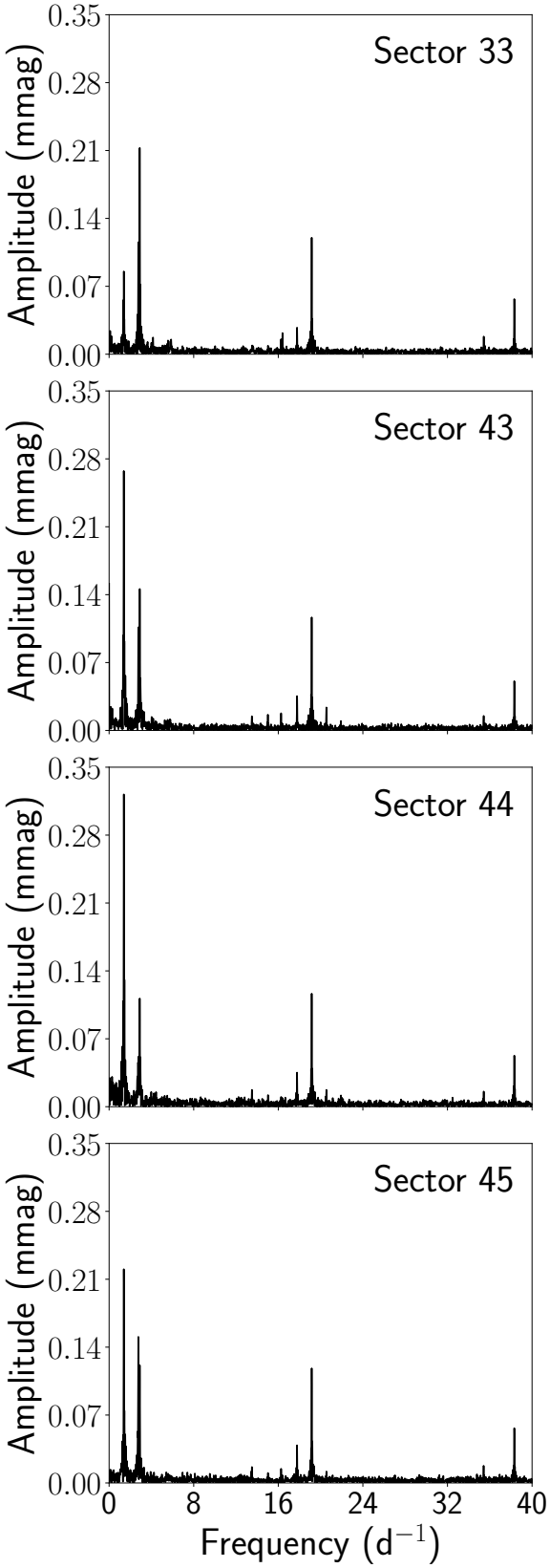

Figure 3. Top: Amplitude spectra of the Sector 33 and 43–45 data for HD 42477. The amplitude variations in the low frequencies, ν_1, ν_2 and ν_3, is evident. The amplitude of the p mode, ν_4, is stable.

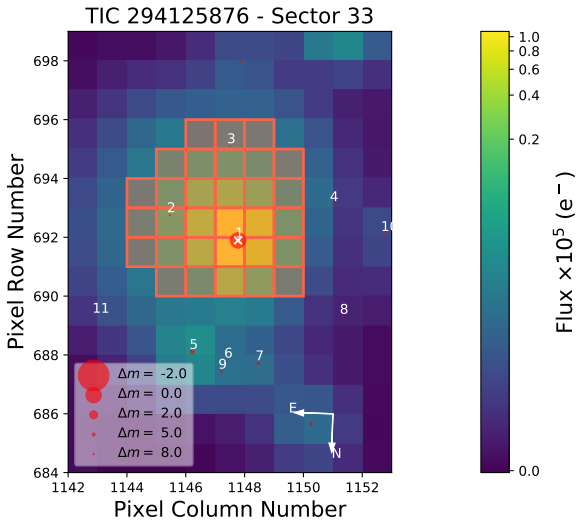

Figure 4. The TESS Target Pixel File of HD 42477 from Sector 33. All pixels within the pipeline mask are marked by shaded red squares. Gaia DR2 sources in the field are marked by red circles, where the size of the circle is a proxy for the Gaia magnitude; specifically, it represents the magnitude differential between HD 42477 and the Gaia source. This plot was created with `tpfplotter` (Aller et al. 2020).

chosen to be consistent with that derived in Section 7, whereas we verified the choice of surface gravity by comparing the observed wings of the hydrogen line profiles with synthetic ones. The best fit was achieved with $\log g = 3.5$. Our choice of $v \sin i$ was also based on a comparison with the observed spectra.

Consequently, we added synthetic spectra of three hypothetical companions to the spectrum of the primary. Companion 1 was assumed to resemble a main sequence star of spectral type F0 ($T_{\rm eff}$ = 7250 K, $\log g = 4.25$) that rotates slowly ($v \sin i = 30$ km s^{-1}). Companion 2 had the same $T_{\rm eff}$ and $\log g$, but rotated more rapidly ($v \sin i = 100$ km s^{-1}), whereas Companion 3 was chosen to match an F3V star ($T_{\rm eff}$ = 6750 K, $\log g = 4.25$) that rotates even more rapidly ($v \sin i = 200$ km s^{-1}). Synthetic composite spectra were computed, and we tested the magnitude difference required to be able to detect such companions in the observed spectra.

We found that Companion 1 would be detectable even if it was 3.5 magnitudes fainter in the V band than the primary star, owing to its sharp spectral lines that are in stark contrast to those of the primary. Companion 2 would be detectable at a V magnitude difference no more than 2.5 magnitudes. Companion 3, however, would escape detection by only being about 1.25 magnitudes fainter in V. This suggests that one of the main factors influencing a putative companion's detectability is its projected rotation rate.

Using the absolute magnitude of HD 42477 as determined in Section 7 and the tables of Pecaut & Mamajek (2013), we estimate that a physical F0V companion would be some 1.8 – 2.1 mag fainter in V. The ultimate conclusion from this part of our study, then, is that our spectra are sufficient to exclude a physical companion to HD 42477 of early to mid-F spectral type if it rotates slower than about 100 km s^{-1} in terms of $v \sin i$, but we would not be able to detect a physically associated rapidly rotating companion star, an optical companion, or a star blended into the TESS pixels of our

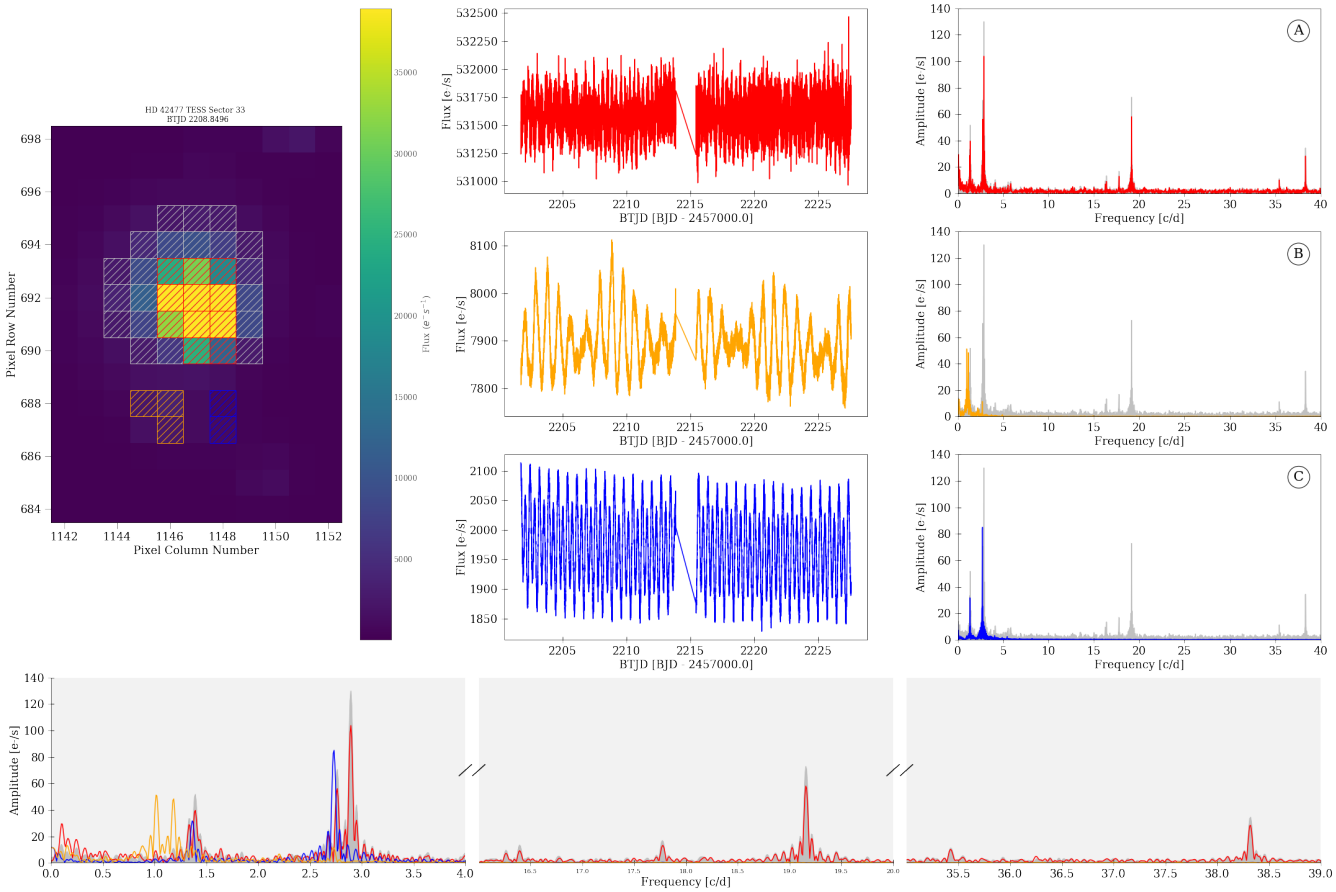

Figure 5. The results of the study of the variability content of the Target Pixel File of HD 42477. Left: the TPF with the aperture masks overplotted; grey – PDCSAP pipeline mask, red – custom mask for HD 42477, orange – custom mask for HD 253085, blue – custom mask for Gaia160. Middle and right: colour-coded light curves created using the corresponding masks corrected with Cotrending Basis Vectors, and their amplitude spectra, for HD 42477 in A, HD 253085 in B and Gaia160 in C. The PDCSAP amplitude spectrum is shown in grey in each panel for comparison. Bottom: 3-panel zoom-in into the ranges of frequencies detected in HD 42477. See the text for more detail.

target at a larger distance. We do note, however, that based on our analysis in Section 5, this last option has largely been ruled out.

7 MODELLING HD 42477

7.1 Global parameters

To obtain starting values of effective temperature, $T_{\rm eff}$, surface gravity, $\log g$, luminosity and radius for modelling HD 42477, we used Strömgren $uvby$ plus Hβ photometry, as well as Johnson BV, along with a variety of other observations.

The Strömgren indices are $b-y = 0.026$, $m_1 = 0.128$, $c_1 = 1.126$, H$\beta = 2.820$. Using the B star calibration of Moon & Dworetsky (1985) (their Figure 3) gives $T_{\rm eff} = 9900$ K, $\log g = 3.4$. Using the A star calibration from the same work by Moon & Dworetsky (their Figure 2) gives $T_{\rm eff} = 7900$ K, $\log g = 3.3$. The reason for this ambiguity is that the Hβ index peaks at A0 (of course, since this is where the Balmer lines have maximum strength by definition of the spectral types). So Hβ drops from its peak on either side of A0. We can decide that the hotter $T_{\rm eff}$ is the correct choice by reference to $b-y = 0.026$. That is calibrated to be 0.0 at A0. Using the calibration of Crawford (1979) gives $b-y = 0.126$ for H$\beta = 2.82$ (his table 1), and a spectral type of A7 for H$\beta = 2.824$ (his table 2). His table suggests A1 or A2 for $b-y = 0.026$. Given that this index includes reddening due to interstellar dust, the corrected reddening-free estimate is hotter.

These Strömgren estimates of $T_{\rm eff} = 9900$ K, $\log g = 3.4$ are the best available for this star. They confirm the A0 classification, and show the star is above the ZAMS, for which $\log g = 4.5$ for A0 stars.

From the Gaia DR3 (Gaia Collaboration et al. 2016, 2022) parallax, 6.427 ± 0.050 mas, we obtain a distance of 155.6 ± 1.2 pc, giving a distance modulus $\mu = 5.960 \pm 0.017$. Photometric measurements of this star in Høg et al. (2000) give $V = 6.036$, $B = 6.050$, and $B-V = 0.014$. The 'Stilism' database[6] (Lallement et al. 2014; Capitanio et al. 2017) gives a colour excess of $E(B-V) = 0.007$ for the direction and at the distance of HD 42477. This results in $(B-V)_0 = 0.007$, consistent with the A0Vnne spectral classification (Cowley et al. 1969). Using the relation among $B-V$, $T_{\rm eff}$, and the Bolometric Correction (BC) as given in Flower (1996), we find $\log T_{\rm eff} = 3.9747$, $T_{\rm eff} = 9434$ K, and BC $= -0.134$.

We then have the absolute bolometric magnitude $M_{\rm bol} =$

[6] https://stilism.obspm.fr

Table 2. Model parameters

$M/\mathrm{M}_\odot$	$\log L/\mathrm{L}_\odot$	$\log T_{\rm eff}$	$\log R/\mathrm{R}_\odot$	$\log g$
2.8	1.940	3.9928	0.508	3.87

-0.080, which corresponds to $\log L/\mathrm{L}_\odot = 1.932$. We rearrange the Stefan-Boltzmann relation, $L = 4\pi R^2\sigma T^4$, and normalise it to the Sun. This yields

$$\log L/\mathrm{L}_\odot = 2\log R/\mathrm{R}_\odot + 4(\log T_{\rm eff} - 3.76185), \quad (1)$$

from which we obtain $\log R/\mathrm{R}_\odot = 0.540$, or $R = 3.5\,\mathrm{R}_\odot$. These global parameters are consistent with a somewhat evolved 2.8-$\mathrm{M}_\odot$ main-sequence model of $(X, Z) = (0.72, 0.014)$.[7] We have selected a model (Table 2) from the main-sequence evolutionary track of 2.8-$\mathrm{M}_\odot$ having parameters consistent with HD 42477.

7.2 r modes

r mode oscillations are global Rossby waves influenced by buoyancy. These oscillations are predominantly horizontal, and the pattern propagates in the direction opposite to the rotation in the co-rotating frame, while they are seen propagating in the same direction of rotation in the inertial frame because the phase speed in the co-rotating frame is slower than the rotation. For this reason, r modes with an azimuthal order $m \geq 1$) have frequencies in the inertial frame between $(m-1)\nu_{\rm rot}$ and $m\nu_{\rm rot}$ (see e.g., Saio et al. 2018, for details)[8].

If we adopt a rotation frequency of $1.42\,\mathrm{d}^{-1}$, the low frequency features of HD 42477 can be fitted with r-mode frequency ranges reasonably well. Fig. 6 shows the expected visibility distributions of r modes when the star is seen with example inclinations i of the rotation axis to the line of sight of 70° (black lines) and 30° (blue lines; solid and dashed lines are for symmetric and anti-symmetric modes with respect to the equator)[9], where the kinetic energy of r modes is assumed to be distributed equally, and the visibility is normalised arbitrarily to 0.1 mmag at the peak of the $m = 1$ r modes.

If energy is equally distributed to r modes, the visibilities of symmetric $m = 1$ modes should be largest. However, the peaks around $2.5 - 2.8\,\mathrm{d}^{-1}$ of HD 42477 indicate much ($\sim 3^2$ times) larger energy is given to $m = 2$ modes. These modes show amplitude modulation on the timescale of months, as discussed in Section 3. This analysis was done using only the Sector 33 data with fixed amplitudes for that sector, so it does not account for the changes in mode amplitude observed in Sectors 43–45.

7.3 Overstable convection modes

Lee & Saio (2020) found that overstable convective core modes excite high order g mode(s) in the envelope, which should be observed as rotational modulations associated with the rotation frequency of the core (i.e., $\sim |m|\nu_{\rm rot}$(cc)). If the rotation frequency of the convective core is assumed to be $1.45\,\mathrm{d}^{-1}$ (and the envelope rotates at $1.42\,\mathrm{d}^{-1}$), an overstable convective mode of $m = -2$ excites envelope g modes at $\sim 2.89\,\mathrm{d}^{-1}$, while an $m = -1$ convective mode excites g modes at $\sim 1.44\,\mathrm{d}^{-1}$. These frequencies are shown by short vertical magenta lines in Fig. 6 (frequency differences among these g modes with an azimuthal order m are too small to be resolved). The $m = -2$ modes are consistent with $\nu_3 = 2.89362\,\mathrm{d}^{-1}$ of HD 42477, while no obvious peaks are present corresponding to the $m = -1$ modes. The reason for the difference may be attributed to the fact that typical growth rates of the latter are about ten times smaller than the former.

We note that using a local mixing length theory we find the convective turnover times between about 30 and 40 d in most part of the convective core. This suggests that convective motions in the core may be responsible for the amplitude modulations of low-frequency peaks of HD 42477, as seen in Fig. 3.

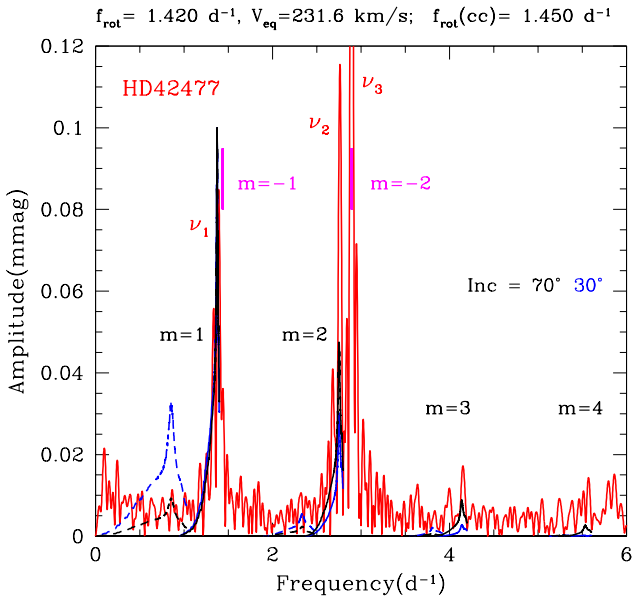

Figure 6. The visibility distributions of r modes (blue and black lines for assumed inclinations of 30° and 70°, respectively) are compared with an amplitude spectrum of HD 42477 (red line). The visibility is obtained under the assumption of energy equi-partition, and an arbitrary normalisation of the maximum of the $m = 1$ modes to be 0.1 mmag. Solid and dashed lines are for r modes whose temperature variations on the surface are, respectively, symmetric and anti-symmetric with respect to the equator. Short vertical magenta lines indicate frequencies of $m = -1$ and -2 prograde g modes excited by an overstable convective mode.

7.3.1 *Angular momentum transfer*

Since overstable convective (OsC) modes in resonance with g modes have amplitudes both in the core and in the envelope, they play a role in angular momentum transfer between the two regions. Prograde OsC modes excited in the core extract angular momentum from the rotating fluid and deposit excess angular momentum to fluids in the envelope where the modes are damped by radiative dissipation. Lee (2021) computed OsC modes of 2-$\mathrm{M}_\odot$, 4-$\mathrm{M}_\odot$ and 20-$\mathrm{M}_\odot$ main-

[7] Main-sequence evolution models (without rotation) were obtained using the MESA code (v.7184; Paxton et al. 2011, 2013, 2015), in which the convective core boundary was determined by the Schwarzschild criterion, elemental diffusion was activated to have a smooth Brunt-Väisälä frequency, and radiation turbulence was also activated to prevent helium settling.

[8] In this paper we adopt the convention that $m > 0$ and $m < 0$ indicate, respectively, retrograde and prograde (in the co-rotating frame) modes.

[9] The actual inclination is probably between these based on the morphology of the weak Hα emission, i.e. the inclination is not very high, nor very low.]

sequence stars and has suggested that the OsC modes can transport angular momentum from the convective core to the envelope by resonantly exciting envelope g modes.

Lee (2021) found that for OsC modes, the timescale corresponding to $\tau(r) \equiv \partial t / \partial \ln \Omega(r)$ in the core is much longer than that in the surface layers. For example, with the results for his 2-$M_\odot$ ZAMS model, assuming $|\delta L_R / L_R| \sim 0.3 \times 10^{-3}$ as suggested by Fig. 2, we obtain $\tau \sim 10^9$ yr in the core and $\tau \sim 10^6$ yr at the surface for $\Omega_s = 0.6 \times \sigma_0$, where $\Omega_s = \Omega(R)$, $\sigma_0 = \sqrt{GM/R^3}$ and G is the gravitational constant. The time scale τ at the surface is much shorter than the lifetime of a 2-$M_\odot$ main sequence star.

In general, as the mass of the star increases, τ becomes shorter. For a 20-$M_\odot$ ZAMS star, for example, assuming the same value as above for $|\delta L_R / L_R|$, we obtain $\tau \sim 10^8$ yr in the core and $\tau \sim 5{\times}10^4$ yr at the surface. For the oscillation amplitudes at the surface that we assume, τ in the core is shorter than the lifetime of a 20-$M_\odot$ main sequence star. Note that the timescale τ is inversely proportional to $(\delta L_R / L_R)^2$, the square of the amplitude.

7.4 p modes

Since HD 42477 is hotter than the blue boundary of the δ Sct instability range in the HR diagram, no p modes in this star are thought to be excited by the kappa mechanism in the second He ionization zone, in contradiction to the TESS photometry which detected a p mode(s) in this star. Our spherical models, unsurprisingly, do not show excitation of any p modes. This possibly could be resolved if the equatorial region is deformed (and cooled) due to the centrifugal force.

However, the detected p mode is clearly coupled to the g modes, which we suggest are themselves excited by overstable convective core modes. We conjecture that the single p mode is driven by coupling with the g modes, or that the oblateness of this rapidly rotating star permits driving by He II ionization in the equatorial region. Both of these are possible explanations for the observed p mode excitation in stars between the β Cep and δ Sct instability strips.

8 HD 42477 AS A CLASSICAL BE STAR

As mentioned in Sec. 2, HD 42477 is a late-type classical Be star, and displays all of the typical hallmarks of a star belonging to this population. Archival spectroscopy from the Be Star Spectra (BeSS) database (Neiner et al. 2011) taken between 2007 and 2022 show that the disk was already weak in 2007 (with the double-peaked emission in Hα reaching only up to ~0.85 in continuum units within the broader absorption profile), and that it had been steadily dissipating through at least the end of the TESS observations considered here. This is corroborated by the series of echelle spectra taken on 8 nights between 2021 May 07 – 2021 Dec 01 (which covered the timespan of TESS sectors 43, 44 and 45) that were used also to check for the presence of a binary companion (see Sec. 6). This indicates that there was no circumstellar activity related to ongoing stellar mass ejection that might otherwise contaminate the variations seen by TESS, so that all photometric variability is stellar in origin, i.e. pulsational. Further, such a weak disk (as is typical for the least massive Be stars) should produce virtually no excess continuum flux at visible wavelengths (Vieira et al. 2017) so that the derivation of the stellar parameters in Sec. 7.1 should be wholly unaffected by the disk.

The most consequential aspect of HD 42477 being a classical Be star lies in the pulsational properties of Be stars at large. Space photometry has revealed that virtually all Be stars pulsate (Rivinius et al. 2016; Semaan et al. 2018; Labadie-Bartz et al. 2022). Indeed, multi-mode, non-radial pulsation is ubiquitous in Be stars, and evidence is mounting that pulsation is a key ingredient in the mass ejection process (Baade et al. 2018b,a; Richardson et al. 2021). By far the most common feature of Be stars observed from space is the presence of two main frequency groups, one of which is typically located between about $1 - 2\,\mathrm{d}^{-1}$, with the second at about twice the frequency of the first, although additional frequencies, in groups or not, often do exist. Different modes may be so closely spaced in frequency that they are unresolved in a single TESS sector, so that their amplitude appears to change from one sector to the next (modulated by the beat envelope). The low-frequency signals in HD 42477 are therefore completely typical for a Be star, supporting the hypothesis that they originate in the rapidly-rotating A0 star (and not a putative companion).

9 CONCLUSIONS

We set out to disprove the conjecture that the p-mode pulsators that appear to lie between the β Cep and δ Sct instability strips are all the result of incorrect determinations of $T_{\rm eff}$, or contamination by a background star or orbital companion. We performed a thorough study of the background stars and also searched for an orbital companion in the spectrum of HD 42477, an A0Vnne star for which the TESS photometry definitely shows a single p mode coupled to lower frequency g modes. No previous study has ruled out the possibility of an orbital companion as the source of the p mode(s) in any star in the range between these two p-mode instability strips. We have almost succeeded, leaving only the possibility of a rapidly rotating, early F companion as the source of the pulsation frequencies. The typical δ Sct star with these characteristics is a multi-mode pulsator; a single p mode in such a star such as this is improbable. And, as we pointed out in Sec. 8 above, virtually all Be stars also show g modes, thus it is highly improbable that the g modes could be in a companion to HD 42477 on this basis.

Given the improbability of a rapidly rotating, early F, singly-periodic δ Sct companion to HD 42477, and given the improbability of an A0Vnne star *not* showing g modes, we have demonstrated that one star in the temperature range between the β Cep and δ Sct stars pulsates with a p mode, thus disproving the conjecture that all such stars might be explained by temperature uncertainties, binary companions, or contamination by background pulsators. This is the first time that such a proof has been given, probably because doing so is a lot of work. Given the fraction of such stars found in this range by Degroote et al. (2009), Bowman & Kurtz (2018) and by the examination of thousands of B and A stars by Balona & Ozuyar (2020), we concur that there are p mode pulsators in the temperature range between the β Cep and γ Dor instability strips.

Through our modelling we have shown the presence of both g modes and r modes in HD 42477, thus demonstrating g mode pulsation in a star cooler than the SPB theoretical instability strip. While it has not yet been shown, visual inspection of *Kepler* and TESS light curves of Be stars indicates to us that r modes are commonly excited in these stars.

The coupling of the g modes and a p mode in HD 42477, plus theoretical understanding of overstable convective core modes as a source of excitation of g modes (such as in the recent work of Lee & Saio 2020; Lee 2021) suggests that mode coupling is important in understanding mode excitation. New calculations of the boundaries

of the instability strips of β Cep, SPB, δ Sct and γ Dor stars with the inclusion of mode coupling may elucidate the presence of pulsators between the currently defined instability strips.

ACKNOWLEDGEMENTS

The authors would like to thank Keaton Bell for illuminating discussions about the contamination analysis.

This work has been partially supported by the Polish National Science Center (NCN) grants 2015/18/A/ST9/00578 and 2021/43/B/ST9/02972 to GH. J.L.-B. acknowledges support from FAPESP (grant 2017/23731-1). This paper includes data collected by the TESS mission, specifically through Guest Investigator Programs G03186 (PI: Labadie-Bartz) and G04067 (PI: Wisniewski). Funding for TESS is provided by NASA's Science Mission Directorate. Resources used in this work were provided by the NASA High End Computing (HEC) Program through the NASA Advanced Supercomputing (NAS) Division at Ames Research Center for the production of the SPOC data products.

This work has made use of observations from the LCOGT network, and also has made use of data from the European Space Agency (ESA) mission *Gaia* (`https://www.cosmos.esa.int/gaia`), processed by the *Gaia* Data Processing and Analysis Consortium (DPAC, `https://www.cosmos.esa.int/web/gaia/dpac/consortium`). Funding for the DPAC has been provided by national institutions, in particular the institutions participating in the *Gaia* Multilateral Agreement. This research made use of Lightkurve, a Python package for Kepler and TESS data analysis (Lightkurve Collaboration, 2018), and `tpfplotter` by J. Lillo-Box (publicly available in www.github.com/jlillo/tpfplotter), which also made use of the python packages `astropy`, `lightkurve`, `matplotlib` and `numpy`.

DATA AVAILABILITY

The data underlying this article will be shared on reasonable request to the authors.

REFERENCES

Aerts C., 2021, Reviews of Modern Physics, 93, 015001
Aerts C., Christensen-Dalsgaard J., Kurtz D. W., 2010, Asteroseismology. Astronomy and Astrophysics Library. Springer Science+Business Media B.V.
Aller A., Lillo-Box J., Jones D., Miranda L. F., Barceló Forteza S., 2020, A&A, 635, A128
Baade D., et al., 2018a, in Wade G. A., Baade D., Guzik J. A., Smolec R., eds, Vol. 8, 3rd BRITE Science Conference. pp 69–76 (`arXiv:1708.08413`)
Baade D., et al., 2018b, A&A, 610, A70
Bai Y., Liu J., Bai Z., Wang S., Fan D., 2019, AJ, 158, 93
Balona L. A., Ozuyar D., 2020, MNRAS, 493, 5871
Bowman D. M., Kurtz D. W., 2018, MNRAS, 476, 3169
Bowman D. M., et al., 2019, Nature Astronomy, 3, 760
Bowman D. M., Burssens S., Simón-Díaz S., Edelmann P. V. F., Rogers T. M., Horst L., Röpke F. K., Aerts C., 2020, A&A, 640, A36
Brown T. M., et al., 2013, PASP, 125, 1031
Capitanio L., Lallement R., Vergely J. L., Elyajouri M., Monreal-Ibero A., 2017, A&A, 606, A65
Cowley A., Cowley C., Jaschek M., Jaschek C., 1969, AJ, 74, 375
Crawford D. L., 1979, AJ, 84, 1858
Degroote P., et al., 2009, A&A, 506, 471
Dupret M. A., Grigahcène A., Garrido R., Gabriel M., Scuflaire R., 2004, A&A, 414, L17
Dupret M. A., Grigahcène A., Garrido R., Gabriel M., Scuflaire R., 2005, A&A, 435, 927
Flower P. J., 1996, ApJ, 469, 355
Gaia Collaboration et al., 2016, A&A, 595, A1
Gaia Collaboration et al., 2022, arXiv e-prints, p. arXiv:2208.00211
Gray R. O., Corbally C. J., 1994, AJ, 107, 742
Grigahcène A., Dupret M. A., Gabriel M., Garrido R., Scuflaire R., 2005, A&A, 434, 1055
Grigahcène A., et al., 2010, ApJ, 713, L192
Guzik J. A., Kaye A. B., Bradley P. A., Cox A. N., Neuforge C., 2000, ApJ, 542, L57
Høg E., et al., 2000, A&A, 355, L27
Houdek G., Dupret M.-A., 2015, Living Reviews in Solar Physics, 12, 8
Kahraman Aliçavuş F., Poretti E., Catanzaro G., Smalley B., Niemczura E., Rainer M., Handler G., 2020, MNRAS, 493, 4518
Kurtz D. W., 1985, MNRAS, 213, 773
Kurtz D. W., 2022, ARA&A, 60, 31
Kurtz D. W., Shibahashi H., Murphy S. J., Bedding T. R., Bowman D. M., 2015, MNRAS, 450, 3015
Labadie-Bartz J., et al., 2017, AJ, 153, 252
Labadie-Bartz J., Carciofi A. C., Henrique de Amorim T., Rubio A., Luiz Figueiredo A., Ticiani dos Santos P., Thomson-Paressant K., 2022, AJ, 163, 226
Lallement R., Vergely J. L., Valette B., Puspitarini L., Eyer L., Casagrande L., 2014, A&A, 561, A91
Lee U., 2021, MNRAS, 505, 1495
Lee U., Saio H., 2020, MNRAS, 497, 4117
Lightkurve Collaboration et al., 2018, Lightkurve: Kepler and TESS time series analysis in Python, Astrophysics Source Code Library (ascl:1812.013)
Moe M., Di Stefano R., 2017, ApJS, 230, 15
Moon T. T., Dworetsky M. M., 1985, MNRAS, 217, 305
Mowlavi N., Barblan F., Saesen S., Eyer L., 2013, A&A, 554, A108
Murphy S. J., Moe M., Kurtz D. W., Bedding T. R., Shibahashi H., Boffin H. M. J., 2018, MNRAS, 474, 4322
Murphy S. J., Hey D., Van Reeth T., Bedding T. R., 2019, MNRAS, 485, 2380
Neiner C., de Batz B., Cochard F., Floquet M., Mekkas A., Desnoux V., 2011, AJ, 142, 149
Paxton B., Bildsten L., Dotter A., Herwig F., Lesaffre P., Timmes F., 2011, ApJS, 192, 3
Paxton B., et al., 2013, ApJS, 208, 4
Paxton B., et al., 2015, ApJS, 220, 15
Pecaut M. J., Mamajek E. E., 2013, ApJS, 208, 9
Richardson N. D., et al., 2021, MNRAS, 508, 2002
Rivinius T., Baade D., Carciofi A. C., 2016, A&A, 593, A106
Saio H., Kurtz D. W., Murphy S. J., Antoci V. L., Lee U., 2018, MNRAS, 474, 2774
Salmon S. J. A. J., Montalbán J., Reese D. R., Dupret M. A., Eggenberger P., 2014, A&A, 569, A18
Semaan T., Hubert A. M., Zorec J., Gutiérrez-Soto J., Frémat Y., Martayan C., Fabregat J., Eggenberger P., 2018, A&A, 613, A70
Sullivan P. W., et al., 2015, ApJ, 809, 77
Szewczuk W., Daszyńska-Daszkiewicz J., 2017, MNRAS, 469, 13
Van Reeth T., Tkachenko A., Aerts C., 2016, A&A, 593, A120
Vieira R. G., Carciofi A. C., Bjorkman J. E., Rivinius T., Baade D., Rímulo L. R., 2017, MNRAS, 464, 3071
White T. R., et al., 2017, MNRAS, 471, 2882

This paper has been typeset from a TEX/LATEX file prepared by the author.